ISSN 0915-633X

INTERNATIONAL ATOMIC ENERGY AGENCY

**FOURTEENTH INTERNATIONAL CONFERENCE ON PLASMA PHYSICS AND CONTROLLED NUCLEAR FUSION RESEARCH**

Würzburg, Germany, 30 September – 7 October 1992

**IAEA-CN-56/D-4-20**

# NATIONAL INSTITUTE FOR FUSION SCIENCE

## *K*-$\epsilon$ Model of Anomalous Transport in Resistive Interchange Turbulence

H. Sugama, M. Okamoto and M. Wakatani

(Received – Aug. 25, 1992)

NIFS-170 Sep. 1992



**RESEARCH REPORT NIFS Series**

INTERNATIONAL ATOMIC ENERGY AGENCY

**FOURTEENTH INTERNATIONAL CONFERENCE ON PLASMA PHYSICS AND CONTROLLED NUCLEAR FUSION RESEARCH**

Würzburg, Germany, 30 September – 7 October 1992

IAEA-CN-56/D-4-20

# $K$-$\epsilon$ MODEL OF ANOMALOUS TRANSPORT IN RESISTIVE INTERCHANGE TURBULENCE

H. SUGAMA and M. OKAMOTO

*National Institute for Fusion Science, Chikusaku, Nagoya 464-01, Japan*

M. WAKATANI

*Plasma Physics Laboratory, Kyoto University, Uji, Kyoto 611, Japan*

**KEYWORDS:** resistive interchange turbulence, anomalous transport, $K$-$\epsilon$ model

# $K$-$\epsilon$ MODEL OF ANOMALOUS TRANSPORT IN RESISTIVE INTERCHANGE TURBULENCE


## ABSTRACT

A $K$-$\epsilon$ anomalous transport model for resistive interchange turbulence is presented and applied to the transport analysis of ECH plasmas in Heliotron E. In this model, the turbulent kinetic energy $K \equiv \frac{1}{2}\langle\tilde{v}^2\rangle$ and its viscous dissipation rate $\epsilon$ characterize the local turbulence and the anomalous transport coefficient is given by $D \sim K^2/\epsilon$, which has some nonlocal properties not included in the conventional expressions since their temporal and spatial variations are determined by taking into account the transport of the turbulent energy itself. In the case of the homogeneous turbulence where the anomalous transport may be described in terms of the local plasma parameters, the dimensional analysis applied to our model yields the two types of local parameter expressions of the anomalous diffusivity in the high and low collisional cases. We find a familiar diffusivity for the resistive interchange turbulence derived in the high collisional case and we have another one similar to the gyro-reduced Bohm (GRB) diffusivity in the low collisional case. However, it is shown from the transport simulation using our model that, in the region where the turbulence inhomogeneity is significant, the anomalous diffusivity deviates from the local parameter expression due to the transport terms in the $K$-$\epsilon$ equations. Our model explains the experimental results consistently in that it gives the GRB or LHD scaling for the energy confinement time and reproduces the experimentally obtained profile of the anomalous diffusivity which has large values in the peripheral region in contrast with the GRB model.


## 1. INTRODUCTION

Conventional treatments for anomalous transport have been based on the local transport coefficients ($D$ or $\chi$) which are expressed as functions of local plasma parameters such as local density $n$, temperature $T$, magnetic field $B$ and a number of gradient scale length $L_n$, $L_T$, $L_s, \cdots$ :

$$D \text{ or } \chi = F(n, T, B, L_n, L_T, L_s, \cdots).$$

These treatments assume that the mixing length $l$ and the time scale $\tau$ of the turbulence responsible for the anomalous transport are determined by the local plasma parameters.

However it is possible that the turbulence structure has nonlocal nature and the validity of the expression for the local transport coefficients as given above is limited.

Here we present a $K$-$\epsilon$ type model for the analysis of anomalous transport in the resistive interchange turbulence. A $K$-$\epsilon$ model was originally proposed for modeling the turbulent (or eddy) viscosity of the large Reynolds number turbulent shear flow [1]. In the $K$-$\epsilon$ model the turbulent kinetic energy $K \equiv \frac{1}{2}\langle\tilde{v}^2\rangle$ and its viscous dissipation rate $\epsilon$ characterize the local turbulence spectral structure and their temporal and spatial variations are governed by transport equations. The turbulent transport coefficient is given by $D \sim K^2/\epsilon$, which has some nonlocal properties not included in the conventional expressions since the mixing length $l \sim K^{3/2}/\epsilon$, the turbulent time scale $\tau \sim K/\epsilon$ and the turbulent transport coefficient $D \sim l^2/\tau \sim K^2/\epsilon$ are determined not locally but globally by the solution of $K$-$\epsilon$ transport equations.

The resistive interchange turbulence has been extensively studied as a cause of anomalous transport in the peripheral region of stellarator plasmas [2,3]. The $K$-$\epsilon$ equations for the resistive interchange turbulence have the turbulent energy production terms, which are given by the pressure gradient multiplied by the average magnetic curvature, the viscous and Joule dissipation terms, and the transport terms. In the case of the homogeneous turbulence, the transport terms vanish and the anomalous transport may be well described in terms of the local plasma parameters. However, when the turbulence is significantly inhomogeneous, the anomalous diffusivity deviates from the local parameter expression due to the transport terms in the $K$-$\epsilon$ equations.

## 2. $K$-$\epsilon$ ANOMALOUS TRANSPORT MODEL

The $K$-$\epsilon$ model for anomalous transport in resistive interchange turbulence was derived in Ref.[4] by applying two-scale direct-interaction approximation (TSDIA) [5] to the resistive magnetohydrodymamical (MHD) equations. Assuming that the mean velocity vanishes $\langle\boldsymbol{v}\rangle = 0$ and that there is the inhomogeneity of turbulence only in the minor radial direction, statistical analyses of the resistive MHD equations show that the equations governing the turbulent kinetic energy $K \equiv \frac{1}{2}\langle\tilde{v}^2\rangle$ and its dissipation rate $\epsilon$ are written as follows,

$$\frac{\partial K}{\partial t} = P_K - \epsilon - \epsilon_J + T_K \tag{1}$$

$$\frac{\partial \epsilon}{\partial t} = C_{\epsilon 1}\frac{\epsilon}{K}P_K - C_{\epsilon 2}\frac{\epsilon^2}{K} - C_{\epsilon J}\frac{\epsilon\epsilon_J}{K} + T_\epsilon. \tag{2}$$

where $\epsilon_J$ denotes the Joule dissipation term and the turbulent energy production term $P_K$, the transport terms $T_K$ and $T_\epsilon$ are given by

$$P_K = \langle \tilde{p}\tilde{\boldsymbol{v}} \rangle \cdot \frac{1}{\rho_m} \frac{d\Omega}{dr} \tag{3}$$

$$T_K = \frac{1}{r}\frac{\partial}{\partial r}\left( rC_K \frac{K^2}{\epsilon}\frac{\partial K}{\partial r}\right), \qquad T_\epsilon = \frac{1}{r}\frac{\partial}{\partial r}\left( rC_\epsilon \frac{K^2}{\epsilon}\frac{\partial \epsilon}{\partial r}\right) \tag{4}$$

Here $\rho_m$ denotes the mass density, $c$ the light velocity in the vacuum, $\eta$ the resistivity, $B$ the magnitude of the magnetic field, and $d\Omega/dr$ the average magnetic curvature. As seen from (3), the turbulent energy production is in the form of the product of the flux and the centrifugal force due to the average magnetic curvature. The turbulent pressure flux $\langle \tilde{p}\tilde{\boldsymbol{v}} \rangle$ is expressed in terms of the mean pressure gradient $dP/dr$ and the turbulent diffusivity $D_p$ as

$$\langle \tilde{p}\tilde{\boldsymbol{v}} \rangle = -D_p \frac{dP}{dr} = -C_p \frac{K^2}{\epsilon}\frac{dP}{dr}. \tag{5}$$

In the same manner as in (5), the turbulent diffusivity for passive scalars in the turbulent velocity field is given by

$$D_\theta = C_\theta \frac{K^2}{\epsilon}. \tag{6}$$

$C_K$, $C_\epsilon$, $C_{\epsilon 1}$, $C_{\epsilon 2}$, $C_{\epsilon J}$, $C_p$, and $C_\theta$ are non-dimensional constants, which are determined empirically or theoretically from TSDIA.

With the electrostatic approximation, the Joule dissipation term $\epsilon_J = \eta \tilde{J}^2/\rho_m$ can be expressed in terms of $K$ and $\epsilon$ as follows. For high collision frequencies such that $L_s^2 m_e \nu_e T_e > \tau (\sim K/\epsilon)$, we have

$$\epsilon_J = C_J \frac{B_0^2}{\rho_m c^2 \eta L_s^2}\frac{K^4}{\epsilon^2} \qquad \text{for} \quad L_s^2 \frac{m_e \nu_e}{T_e} > \tau \tag{7}$$

where $L_s$ is a magnetic shear length and $C_J$ a non-dimensional numerical constant. Here we used the Ohm's law $\tilde{J} \sim \eta^{-1} k_\parallel \tilde{\phi}$ and estimated that $K \sim \tilde{v}^2 \sim (ck_\perp \tilde{\phi}/B)^2$ and $k_\parallel/k_\perp \sim l/L_s$. On the other hand, for low collision frequencies such that $L_s^2 m_e \nu_e/T_e < \tau$, we need to take account of the adiabaticity of electron response to potential fluctuations to evaluate $\epsilon_J$. From the balance between the time scales of the electron parallel conduction and the potential fluctuation $k_\parallel^2 T_e/(m_e \nu_e) \sim \tau^{-1}$ with $k_\parallel \sim k_\perp \Delta/L_s$, the width of the non-adiabatic layer $\Delta$ is given by $k_\perp^2 \Delta^2 \sim L_s^2 (m_e \nu_e/T_e)\tau^{-1}$. Therefore, in this low collisional case, $\Delta$ becomes smaller than the turbulent mixing length $l \sim K^{3/2}/\epsilon$. Using the generalized Ohm's law $\tilde{J} \sim (T_e/e\eta) k_\parallel (\tilde{n}/n_0 - e\tilde{\phi}/T_e)$ and noting that we have the Boltzmann relation

$\tilde{n}/n_0 \sim e\phi/T_e$ outside the non-adiabatic layer and $\tilde{n}/n_0 < e\phi/T_e$ inside it, we obtain $\tilde{J}^2 \sim \eta^{-2}(\Delta/L_s)^2(k_\perp\tilde{\phi})^2$. From these relations, we have

$$\epsilon_J = C_J' \frac{1}{\rho_s^2} \frac{K^3}{\epsilon} \qquad \text{for} \quad L_s^2 \frac{m_e \nu_e}{T_e} < \tau \tag{8}$$

where $C_J'$ is a numerical constant and $\rho_s = c\sqrt{m_i T_e}/(eB_0)$ the ion Larmor radius at the electron temperature.

If the profiles of the mean pressure gradient $dP/dr$ and the magnetic curvature $d\Omega/dr$ are given, we can obtain the turbulent diffusivity (6) by solving the $K$-$\epsilon$ transport equations (1) and (2) with proper boundary conditions imposed. The self-consistent model for the analysis of anomalous transport is obtained by combining the $K$-$\epsilon$ equations with the transport equations for the density and temperature. The profiles of the density and temperature affect the turbulence through the production and dissipation terms in the $K$-$\epsilon$ equations while the turbulence has dominant effects on the transport of the density and temperature through the anomalous diffusivities. The diffusion terms given by (4) describe the radial propagation of the turbulence which have not been taken into account by the conventional anomalous transport model.

## 3. SCALING IN TERMS OF LOCAL PARAMETERS

Here, we consider the stationary case in which the transport term in the turbulent energy can be neglected so that the energy production and dissipation terms are balanced with each other. Even then, the turbulent energy flux does not need to vanish although it should have a constant value. Then we obtain from (1), (3) and (5),

$$C_p \left( \frac{-1}{\rho_m} \frac{dP}{dr} \frac{d\Omega}{dr} \right) \frac{K^2}{\epsilon} - \epsilon - \epsilon_J = 0 \tag{9}$$

In this case, as seen from (7)–(9), it can be assumed that the turbulence property is characterized locally by two parameters, which are for high collision frequencies ($L_s^2 m_e \nu_e / T_e > \tau$),

$$\frac{-1}{\rho_m} \frac{dP}{dr} \frac{d\Omega}{dr}, \qquad \frac{\rho_m c^2 \eta L_s^2}{B_0^2} \tag{10}$$

and for low collision frequencies ($L_s^2 m_e \nu_e / T_e < \tau$),

$$\frac{-1}{\rho_m} \frac{dP}{dr} \frac{d\Omega}{dr}, \qquad \rho_s. \tag{11}$$

In the case considered here, the turbulence is regarded as locally homogeneous and these parameters need to be nearly constant. When the variation of the parameters is large, the turbulence can be no longer homogeneous and the turbulent energy transport term becomes important so that the assumption given above is not valid. The first parameter of (10) or (11) is written as $-P'\Omega'/\rho_m \sim c_s^2/(L_pL_c)$ and has a dimension of square frequency, which gives the characteristic time scale $\sqrt{L_pL_c}/c_s$ of the turbulence driven by the pressure gradient and the magnetic curvature. Here $dP/dr = P' = -P/L_p$, $d\Omega/dr = \Omega' = 1/L_c$ and $c_s = \sqrt{T_e/m_i}$ are used and $T_e \geq T_i$ is assumed.

We have the following scaling in terms of the above local parameters from the dimensional analysis. First, in the high collisional case,

$$\begin{aligned} &K \sim c^2\eta\rho_m^{-1/2}(-P'\Omega')^{3/2}L_s^2/B_0^2, && l \sim K^{3/2}/\epsilon \sim c\eta^{1/2}(-\rho_m P'\Omega')^{1/4}L_s/B_0^2, \\ &\epsilon \sim c^2\eta\rho_m^{-1}(-P'\Omega')^2L_s^2/B_0^2, && \tau \sim K/\epsilon \sim (-P'\Omega'/\rho_m)^{-1/2} \sim (c_s/\sqrt{L_pL_c})^{-1}. \end{aligned} \tag{12}$$

Then we obtain the anomalous diffusivity $D$ as

$$D \sim \frac{K^2}{\epsilon} \sim \frac{l^2}{\tau} \sim \frac{c^2\eta(-P'\Omega')L_s^2}{B_0^2} \sim D_{cl}\frac{L_s^2}{L_pL_c} \tag{13}$$

where we used the classical diffusivity $D_{cl} = c^2\eta P/B_0^2$. Equation (13) is the same expression as that of the anomalous diffusivity for the resistive interchange turbulence obtained from the reduced MHD equations using the dimensional analysis or the scale invariance technique. Using the time scale $\tau \sim \sqrt{L_pL_c}/c_s$, we can write the condition for the high collisional case as $L_s^2 m_e\nu_e/T_e > \sqrt{L_pL_c}/c_s$.

Next, in the same way as above, we obtain the scaling in the low collisional case as follows

$$\begin{aligned} &K \sim \rho_s^2c_s^2/L_pL_c, && l \sim K^{3/2}/\epsilon \sim \rho_s, \\ &\epsilon \sim \rho_s^2c_s^3/(L_pL_c)^{3/2}, && \tau \sim K/\epsilon \sim (c_s/\sqrt{L_pL_c})^{-1}. \end{aligned} \tag{14}$$

which gives the anomalous diffusivity $D$ as

$$D \sim \frac{K^2}{\epsilon} \sim \frac{l^2}{\tau} \sim \frac{\rho_s^2c_s}{\sqrt{L_pL_c}} \sim D_B\frac{\rho_s}{\sqrt{L_pL_c}} \tag{15}$$

where we used the Bohm diffusivity $D_B = \rho_sc_s = cT_e/(eB_0)$. Equation (15) has the form of the gyro-reduced Bohm (GRB) diffusivity [6] which is the Bohm diffusivity multiplied by the factor $\rho_s/\sqrt{L_pL_c}$. The condition for the low collisional case is written as $L_s^2m_e\nu_e/T_e < \sqrt{L_pL_c}/c_s$.

## 4. TRANSPORT SIMULATION OF ECH PLASMAS IN HELIOTRON E

We have combined the $K$-$\epsilon$ anomalous transport model with the transport code for stellarators [7] to simulate ECH plasmas in Heliotron E ($R = 2.2m,\ a = 0.2m$) [8,9].

The anomalous particle diffusivity $D$ is given by (6). We have assumed that both the electron and ion thermal diffusivities are given by the same expression $\chi_e = \chi_i = \frac{5}{2}D$. In our simulations, the averaged electron density $\overline{n}_e$, the ECH absorbed power $P_{abs}$ and the magnetic field strength $B$ were scanned in the following ranges: $1 \leq \overline{n}_e \leq 3 \times 10^{19} m^{-3}$, $96 \leq P_{abs} \leq 288 kW$ and $B = 0.95,\ 1.9T$, respectively. We have done numerically the time integration of the electron and ion temperatures, $T_e$, $T_i$ as well as the turbulent energy $K$ and its dissipation rate $\epsilon$ while the electron density profile was fixed. We gave the profiles of the electron density and the absorbed power density as $n_e(r) = n_e(0)\,[\,0.95\,(1 - (r/a)^6) + 0.05\,]$ and $p_{abs}(r) = p_{abs}(0)\,(1 - (r/a)^4)^2$ which fit the experimentally observed results. The average magnetic curvature $d\Omega/dr$ was given from the vacuum magnetic field configuration of Heliotron E since the beta values of the ECH plasmas simulated here are very low. The neoclassical diffusivities were included in our simulations although the effects of the radial electric field and the neutral particles are assumed to be negligible in order to clarify the effects of the anomalous transport. In the parameter regime of the ECH plasmas in Heliotron E, the whole plasma is considered to satisfy the low collision frequency condition and therefore we employed the Joule dissipation term given by (8). The numerical constants used here are $C_K = 0.09$, $C_\epsilon = 0.07$, $C_{\epsilon 1} = C_{\epsilon 2} = C_{\epsilon J} = 1.7$, $C_p = C_\theta = 0.135$ and $C'_J = 0.05$.

After adequate time steps, we obtained the stationary states in which the radial profiles of $T_e$, $T_i$, $K$ and $\epsilon$ did not depend on the initial conditions. Figure 1 shows the radial profile of the anomalous thermal diffusivity obtained by $K$-$\epsilon$ model, $\chi_e^{K\text{-}\epsilon} = \frac{5}{2} C_\theta K^2/\epsilon$, in the stationary state for $\overline{n}_e = 1 \times 10^{19} m^{-3}$, $P_{abs} = 192 kW$ and $B = 1.9T$. In this case, the boundary conditions for $K$ and $\epsilon$ were given such that the energy confinement time took the experimentally observed value. There also shown is the profile of the anomalous diffusivity expressed in terms of the local parameters as in (15), $\chi_e^{local} \equiv C\,(\rho_s/\sqrt{L_p L_c})\,c(T_e + T_i)/eB$, where the value of the numerical coefficient employed in Fig.1 is $C = 0.57$. It can be seen that both of the diffusivities have the same radial dependence in the region $0.1 < r/a < 0.6$ while the discrepancy between their profiles becomes large in the other regions. Especially, in the peripheral region, $\chi_e^{K\text{-}\epsilon}$ increases in approaching the boundary whereas $\chi_e^{local}$ decreases. Figure 2 shows the radial profiles of the turbulent energy production, viscous and Joule dissipations in the same case as in Fig.1. It is found that the production and dissipation occur mostly near the peripheral region where the average magnetic curvature becomes large. In this case, the inward transport of the turbulent energy appears. The ratio of the Joule dissipation to the viscous one increases in the peripheral region due to the decrease in the temperature, which is correlated with the deviation of $\chi_e^{K\text{-}\epsilon}$ from $\chi_e^{local}$ since the ratio between the production, viscous and Joule dissipations need to be homogeneous or constant in order to ensure the validity of the scaling by the local parameters. Thus the local parameter expression poorly predicts the anomalous transport coefficient in the peripheral region where the inhomogeneities of the local parameters in (11) are significant.

In Fig.3, the experimentally obtained thermal diffusivity $\chi_e^{exp}$ in the case corresponding to Fig.1 is compared with the numerically predicted total diffusivity $\chi_e^{total} = \chi_e^{K\text{-}\epsilon} + \chi_e^{neo\text{-}ax} + \chi_e^{ripple}$, where $\chi_e^{neo\text{-}ax}$ and $\chi_e^{ripple}$ denote the neoclassical axisymmetric and non-axisymmetric (ripple) thermal diffusivities, respectively. The disagreement between $\chi_e^{total}$ and $\chi_e^{exp}$ seems to be within the accuracy of the experimental results although the predicted diffusivity $\chi_e^{tot}$ may be relatively smaller than $\chi_e^{exp}$ in the inner region $r < 0.3a$ since there the magnetic curvature is quite small and other turbulence sources are not taken into account in our model. It is seen that the anomalous diffusivity is a dominant contribution to the whole plasma confinement although $\chi_e^{ripple}$ is comparable to $\chi_e^{K\text{-}\epsilon}$ at $0.3 < r/a < 0.5$ and $\chi_e^{neo\text{-}ax}$ is the largest at $r/a < 0.1$.

We have scanned the electron density, the absorbed power and the magnetic field strength in the ranges mentioned earlier. Since we have seen in Fig.1 that the local parameter expression (15) is valid in the regions except for the peripheral and central regions, we adjusted the boundary conditions for $K$ and $\epsilon$ in all the simulations in the above ranges such that the $K$-$\epsilon$ anomalous diffusivity coincide with the local expression at $r = a/2$ : $\chi_e^{K\text{-}\epsilon}(a/2) = \chi_e^{local}(a/2)$. In Fig.4, the energy confinement times $\tau_E^{K\text{-}\epsilon}$ obtained from the simulations are compared with the LHD scaling [10]. It is found that the simulation results are in good agreement with the LHD scaling. This seems to be natural since the thermal diffusivity imposed at $r = a/2$ obeies a type of GRB scaling which gives almost the same energy confinement time as the LHD scaling. Thus our model predicts the experimental results consistently in the two aspects: the first is that it gives the energy confinement time following the GRB or LHD scaling and the second is that it supplements the drawback of the GRB diffusivity, i. e., it reproduces the experimentally observed profile of the anomalous diffusivity which has large values in the peripheral region.

## REFERENCES

[1] BRADSHAW, P., CEBECI T., WHITELAW, J. H., Engineering Calculation Method

for Turbulent Flow, Academic, London (1981) 37.

[2] CARRERAS, B. A., GARCIA, L., DIAMOND, P. H., Phys. Fluids **30** (1987) 1388.

[3] SUGAMA, H., WAKATANI, M., J. Phys. Soc. Jpn. **57** (1988) 2010.

[4] SUGAMA, H., WAKATANI, M., to be published in J. Phys. Soc. Jpn.

[5] YOSHIZAWA, A., Phys. Fluids **27** (1984) 1377.

[6] PERKINS, F. W., in Heating in Toroidal Plasmas (Proc. 4th Int. Symp. Rome, 1984), Vol.2 (1984) 977.

[7] NAKAMURA, Y., WAKATANI, M., Transport Simulation of New Stellarator/Heliotron Devices based on the Neoclassical Ripple Transport associated with an Edge Turbulence, Rep. PPLK-R-24, Plasma Phys. Lab., Kyoto Univ., Uji (1988).

[8] ZUSHI, H., et al., Nucl. Fusion **28** (1988) 1801.

[9] SUDO, S., et al., Nucl. Fusion **31** (1991) 2349.

[10] SUDO, S., et al., Nucl. Fusion **30** (1990) 11.

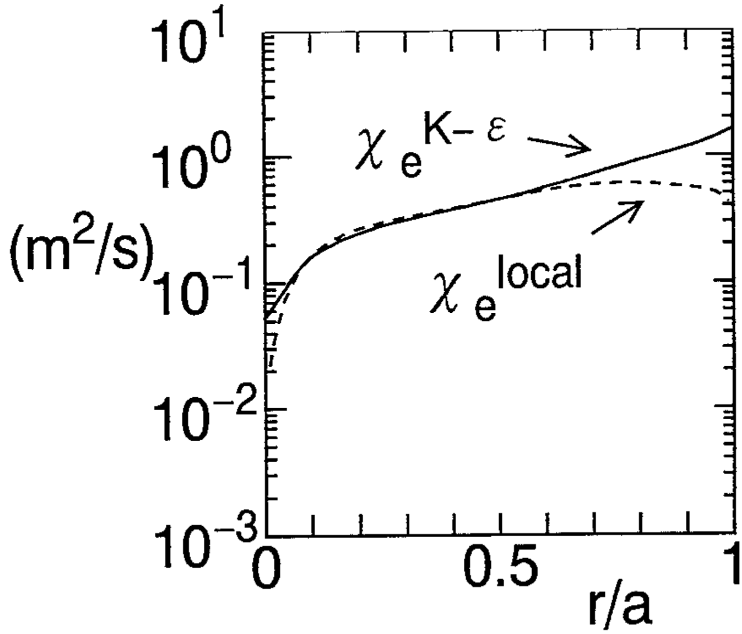


FIG.1. Comparison between the anomalous thermal diffusivity of the $K$-$\epsilon$ model, $\chi_e^{K-\epsilon}$, and that of the local parameter expression, $\chi_e^{local}$.

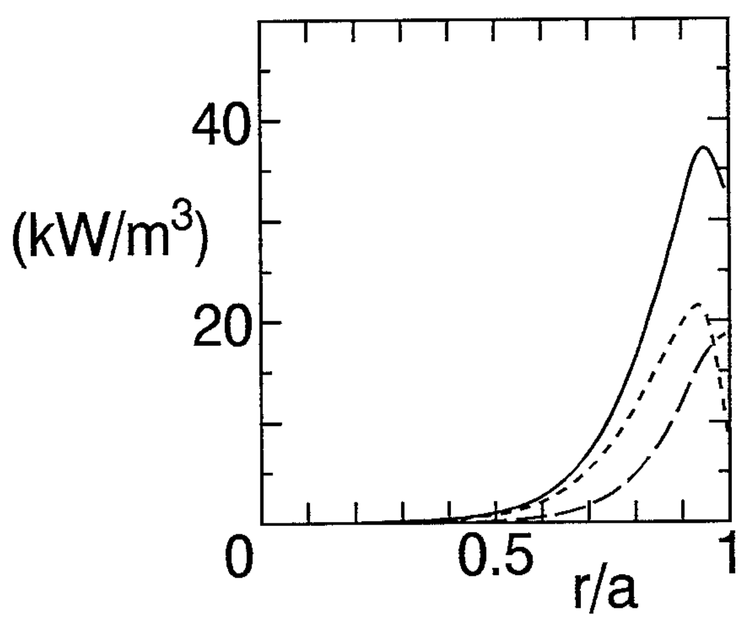


FIG.2. Radial profiles of the turbulent kinetic energy production (solid line), the viscous dissipation (dotted line) and the Joule dissipation (dashed line).

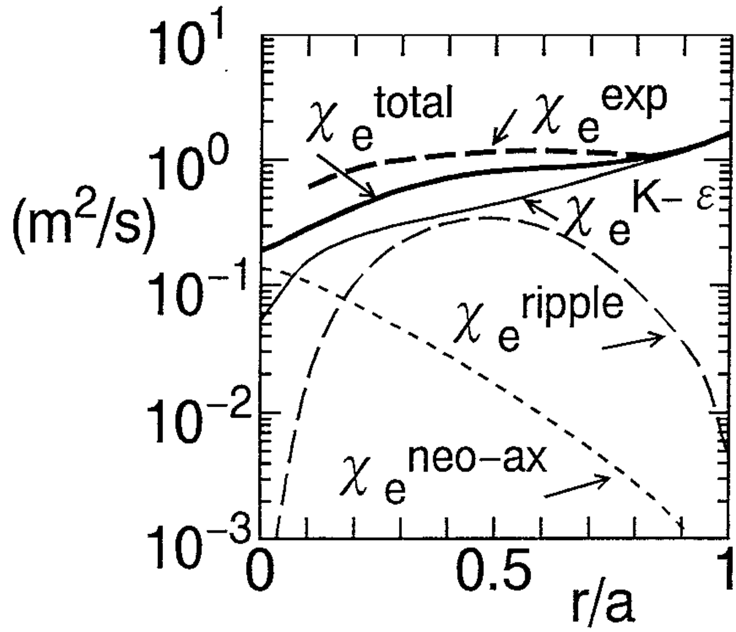


FIG.3. Radial profiles of the neoclassical axisymmetric thermal diffusivity $\chi_e^{neo-ax}$, the neoclassical ripple diffusivity $\chi_e^{ripple}$, the $K$-$\epsilon$ anomalous diffusivity $\chi_e^{K-\epsilon}$, the total diffusivity $\chi_e^{total} = \chi_e^{K-\epsilon} + \chi_e^{neo-ax} + \chi_e^{ripple}$ and the experimentally obtained diffusivity $\chi_e^{exp}$.

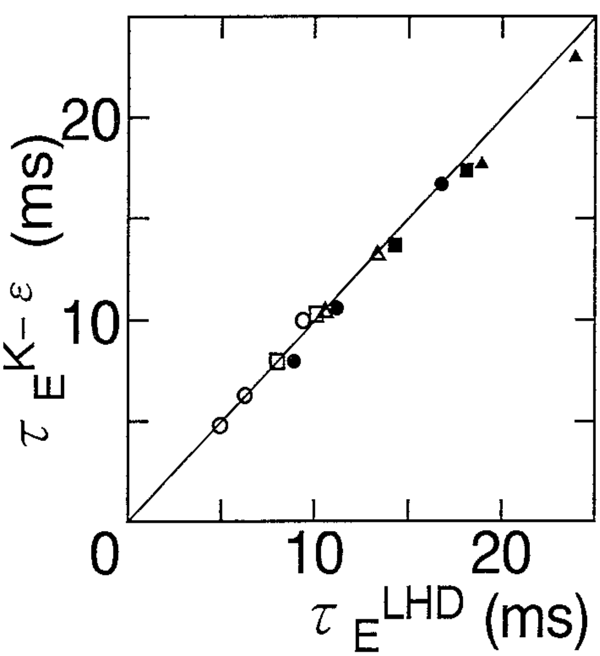


FIG.4. Comparison between the energy confinement times obtained from the simulations using the $K$-$\epsilon$ model, $\tau_E^{K-\epsilon}$, and those of the LHD scaling [10], $\tau_E^{LHD}$.

## Recent Issues of NIFS Series

NIFS-119 T. Yabe and T. Ishikawa, *Two- and Three-Dimensional Simulation Code for Radiation-Hydrodynamics in ICF*; Nov. 1991

NIFS-120 S. Kawata, M. Shiromoto and T. Teramoto, *Density-Carrying Particle Method for Fluid* ; Nov. 1991

NIFS-121 T. Ishikawa, P. Y. Wang, K. Wakui and T. Yabe, *A Method for the High-speed Generation of Random Numbers with Arbitrary Distributions;* Nov. 1991

NIFS-122 K. Yamazaki, H. Kaneko, Y. Taniguchi, O. Motojima and LHD Design *Group, Status of LHD Control System Design ; Dec. 1991*

NIFS-123 Y. Kondoh, *Relaxed State of Energy in Incompressible Fluid and Incompressible MHD Fluid* ; Dec. 1991

NIFS-124 K. Ida, S. Hidekuma, M. Kojima, Y. Miura, S. Tsuji, K. Hoshino, M. Mori, N. Suzuki, T. Yamauchi and JFT-2M Group, *Edge Poloidal Rotation Profiles of H-Mode Plasmas in the JFT-2M Tokamak ;* Dec. 1991

NIFS-125 H. Sugama and M. Wakatani, *Statistical Analysis of Anomalous Transport in Resistive Interchange Turbulence* ;Dec. 1991

NIFS-126 K. Narihara, *A Steady State Tokamak Operation by Use of Magnetic Monopoles* ; Dec. 1991

NIFS-127 K. Itoh, S. -I. Itoh and A. Fukuyama, *Energy Transport in the Steady State Plasma Sustained by DC Helicity Current Drive* ;Jan. 1992

NIFS-128 Y. Hamada, Y. Kawasumi, K. Masai, H. Iguchi, A. Fujisawa, JIPP T-IIU Group and Y. Abe, *New Hight Voltage Parallel Plate Analyzer* ; Jan. 1992

NIFS-129 K. Ida and T. Kato, *Line-Emission Cross Sections for the Charge-exchange Reaction between Fully Stripped Carbon and Atomic Hydrogen in Tokamak Plasma*; Jan. 1992

NIFS-130 T. Hayashi, A. Takei and T. Sato, *Magnetic Surface Breaking in 3D MHD Equilibria of l=2 Heliotron* ; Jan. 1992

NIFS-131 K. Itoh, K. Ichiguchi and S. -I. Itoh, *Beta Limit of Resistive Plasma in Torsatron/Heliotron* ; Feb. 1992

NIFS-132 K. Sato and F. Miyawaki, *Formation of Presheath and Current-Free*

*Double Layer in a Two-Electron-Temperature Plasma* ; Feb. 1992

NIFS-133 T. Maruyama and S. Kawata, *Superposed-Laser Electron Acceleration* Feb. 1992

NIFS-134 Y. Miura, F. Okano, N. Suzuki, M. Mori, K. Hoshino, H. Maeda, T. Takizuka, JFT-2M Group, S.-I. Itoh and K. Itoh, *Rapid Change of Hydrogen Neutral Energy Distribution at L/H-Transition in JFT-2M H-mode ;* Feb. 1992

NIFS-135 H. Ji, H. Toyama, A. Fujisawa, S. Shinohara and K. Miyamoto *Fluctuation and Edge Current Sustainment in a Reversed-Field-Pinch;* Feb. 1992

NIFS-136 K. Sato and F. Miyawaki, *Heat Flow of a Two-Electron-Temperature Plasma through the Sheath in the Presence of Electron Emission;* Mar. 1992

NIFS-137 T. Hayashi, U. Schwenn and E. Strumberger, *Field Line Diversion Properties of Finite β Helias Equilibria;* Mar. 1992

NIFS-138 T. Yamagishi, *Kinetic Approach to Long Wave Length Modes in Rotating Plasmas*; Mar. 1992

NIFS-139 K. Watanabe, N. Nakajima, M. Okamoto, Y. Nakamura and M. Wakatani, *Three-dimensional MHD Equilibrium in the Presence of Bootstrap Current for Large Helical Device (LHD)*; Mar. 1992

NIFS-140 K. Itoh, S. -I. Itoh and A. Fukuyama, *Theory of Anomalous Transport in Toroidal Helical Plasmas;* Mar. 1992

NIFS-141 Y. Kondoh, *Internal Structures of Self-Organized Relaxed States and Self-Similar Decay Phase;* Mar. 1992

NIFS-142 U. Furukane, K. Sato, K. Takiyama and T. Oda, *Recombining Processes in a Cooling Plasma by Mixing of Initially Heated Gas*; Mar. 1992

NIFS-143 Y. Hamada, K. Masai, Y. Kawasumi, H. Iguchi, A. Fijisawa and JIPP T-IIU Group, *New Method of Error Elimination in Potential Profile Measurement of Tokamak Plasmas by High Voltage Heavy Ion Beam Probes;* Apr. 1992

NIFS-144 N. Ohyabu, N. Noda, Hantao Ji, H. Akao, K. Akaishi, T. Ono, H. Kaneko, T. Kawamura, Y. Kubota, S. Morimoto. A. Sagara, T. Watanabe, K. Yamazaki and O. Motojima, *Helical Divertor in the Large Helical Device;* May 1992

NIFS-145 K. Ohkubo and K. Matsumoto, *Coupling to the Lower Hybrid Waves with the Multijunction Grill*; May 1992

NIFS-146 K. Itoh, S. -I.Itoh, A. Fukuyama, S. Tsuji and Allan J. Lichtenberg, *A Model of Major Disruption in Tokamaks*; May 1992

NIFS-147 S. Sasaki, S. Takamura, M. Ueda, H. Iguchi, J. Fujita and K. Kadota, *Edge Plasma Density Reconstruction for Fast Monoenergetic Lithium Beam Probing*; May 1992

NIFS-148 N. Nakajima, C. Z. Cheng and M. Okamoto, *High-n Helicity-induced Shear Alfvén Eigenmodes*; May 1992

NIFS-149 A. Ando, Y. Takeiri, O. Kaneko, Y. Oka, M. Wada, and T. Kuroda, *Production of Negative Hydrogen Ions in a Large Multicusp Ion Source with Double-Magnetic Filter Configuration*; May 1992

NIFS-150 N. Nakajima and M. Okamoto, *Effects of Fast Ions and an External Inductive Electric Field on the Neoclassical Parallel Flow, Current, and Rotation in General Toroidal Systems*; May 1992

NIFS-151 Y. Takeiri, A. Ando, O. Kaneko, Y. Oka and T. Kuroda, *Negative Ion Extraction Characteristics of a Large Negative Ion Source with Double-Magnetic Filter Configuration*; May 1992

NIFS-152 T. Tanabe, N. Noda and H. Nakamura, *Review of High Z Materials for PSI Applications* ; Jun. 1992

NIFS-153 Sergey V. Bazdenkov and T. Sato, *On a Ballistic Method for Double Layer Regeneration in a Vlasov-Poisson Plasma*; Jun. 1992

NIFS-154 J. Todoroki, *On the Lagrangian of the Linearized MHD Equations*; Jun. 1992

NIFS-155 K. Sato, H. Katayama and F. Miyawaki, *Electrostatic Potential in a Collisionless Plasma Flow Along Open Magnetic Field Lines;* Jun. 1992

NIFS-156 O.J.W.F.Kardaun, J.W.P.F.Kardaun, S.-I. Itoh and K. Itoh, *Discriminant Analysis of Plasma Fusion Data*; Jun. 1992

NIFS-157 K. Itoh, S.-I. Itoh, A. Fukuyama and S. Tsuji, *Critical Issues and Experimental Examination on Sawtooth and Disruption Physics*; Jun. 1992

NIFS-158 K. Itoh and S.-I. Itoh, *Transition to H-Mode by Energetic Electrons*; July 1992

NIFS-159 K. Itoh, S.-I. Itoh and A. Fukuyama, *Steady State Tokamak Sustained by Bootstrap Current Without Seed Current*; July 1992

NIFS-160 H. Sanuki, K. Itoh and S.-I. Itoh, *Effects of Nonclassical Ion Losses on Radial Electric Field in CHS Torsatron/Heliotron*; July 1992

NIFS-161 O. Motojima, K. Akaishi, K. Fujii, S. Fujiwaka, S. Imagawa, H. Ji, H. Kaneko, S. Kitagawa, Y. Kubota, K. Matsuoka, T. Mito, S. Morimoto, A. Nishimura, K. Nishimura, N. Noda, I. Ohtake, N. Ohyabu, S. Okamura, A. Sagara, M. Sakamoto, S. Satoh, T. Satow, K. Takahata, H. Tamura, S. Tanahashi, T. Tsuzuki, S. Yamada, H. Yamada, K. Yamazaki, N. Yanagi, H. Yonezu, J. Yamamoto, M. Fujiwara and A. Iiyoshi, *Physics and Engineering Design Studies on Large Helical Device*; Aug. 1992

NIFS-162 V. D. Pustovitov, *Refined Theory of Diamagnetic Effect in Stellarators;* Aug. 1992

NIFS-163 K. Itoh, *A Review on Application of MHD Theory to Plasma Boundary Problems in Tokamaks*; Aug. 1992

NIFS-164 Y.Kondoh and T.Sato, *Thought Analysis on Self-Organization Theories of MHD Plasma*; Aug. 1992

NIFS-165 T. Seki, R. Kumazawa, T. Watari, M. Ono, Y. Yasaka, F. Shimpo, A. Ando, O. Kaneko, Y. Oka, K. Adati, R. Akiyama, Y. Hamada, S. Hidekuma, S. Hirokura, K. Ida, A. Karita, K. Kawahata, Y. Kawasumi, Y. Kitoh, T. Kohmoto, M. Kojima, K. Masai, S. Morita, K. Narihara, Y. Ogawa, K. Ohkubo, S. Okajima, T. Ozaki, M. Sakamoto, M. Sasao, K. Sato, K. N. Sato, H. Takahashi, Y. Taniguchi, K. Toi and T. Tsuzuki, *High Frequency Ion Bernstein Wave Heating Experiment on JIPP T-IIU Tokamak*; Aug. 1992

NIFS-166 Vo Hong Anh and Nguyen Tien Dung, *A Synergetic Treatment of the Vortices Behaviour of a Plasma with Viscosity*; Sep. 1992

NIFS-167 K. Watanabe and T. Sato, *A Triggering Mechanism of Fast Crash in Sawtooth Oscillation*; Sep. 1992

NIFS-168 T. Hayashi, T. Sato, W. Lotz, P. Merkel, J. Nührenberg, U. Schwenn and E. Strumberger, *3D MHD Study of Helias and Heliotron;* Sep. 1992

NIFS-169 N. Nakajima, K. Ichiguchi, K. Watanabe, H. Sugama, M. Okamoto, M. Wakatani, Y. Nakamura and C. Z. Cheng, *Neoclassical Current and Related MHD Stability, Gap Modes, and Radial Electric Field Effects in Heliotron and Torsatron Plasmas;* Sep. 1992